Use of Diastereomeric Interactions To Probe the Inplane Attachment of Water-Soluble Molecules to the Polar Head Groups of Langmuir Films of Cu−α-Amino Acid Complexes

Maria Berfeld,[†] Ivan Kuzmenko,[†] Isabelle Weissbuch,[†] Hagai Cohen,[†] Paul B. Howes,[‡] Kristian Kjaer,[‡] Jens Als-Nielsen,[§] Leslie Leiserowitz,*[,†] and Meir Lahav*[,†]

Department of Materials & Interfaces, The Weizmann Institute of Science, 76100 Rehovot, Israel, Department of Solid State Physics, Risø National Laboratory, DK 4000 Roskilde, Denmark, and Niels Bohr Institute, H. C. Ørsted Laboratory, DK 2100 Copenhagen, Denmark

Received: February 16, 1999

To provide more direct information on the role played by "tailor-made" auxiliary molecules in the early stages of crystal nucleation, the interplay between clusters of polar headgroups of monolayers of the copper complexes *S*−Cu−*S*′ and *S*−Cu−*R*′ and water-soluble copper complexes *S*′−Cu−*S*′ and *R*′−Cu−*R*′ were investigated [where *S* represents enantiomerically pure (*S*)-palmitoyl-*N*$^{\epsilon}$-lysine, and *S*′ and *R*′ represent chiral resolved (*S*) and (*R*) forms of alanine, serine, or valine]. The different monolayers were formed by spreading the amphiphilic (*R*) or (*S*) α-amino acid on an aqueous solution of copper acetate followed by injection of the water-soluble (*S*′) or (*R*′) α-amino acid into the subphase. The surface pressure−molecular area isotherms of the Langmuir monolayers of the two type of complexes (*S*−Cu−*S*′ and *S*−Cu−*R*′) are different, the former being substantially more expanded. The polar headgroups of the *S*−Cu−*S*′ and of the *S*−Cu−*R*′ monolayers transferred onto a solid support assume a *trans* and *cis* configuration, respectively, according to comparative X-ray photoelectron spectroscopy (XPS) studies with appropriate *cis* and *trans* three-dimensional (3-D) α-amino acid Cu complexes. A grazing incidence X-ray diffraction (GIXD) analysis demonstrated that the *S*−Cu−*S*′ and *S*−Cu−*R*′ monolayers have different 2-D crystal structures, in keeping with the XPS results. A model is presented suggesting that the water-soluble *S*′−Cu−*S*′ copper complexes are enantioselectively bound to the periphery of the domains of the *cis S*−Cu−*S*′ monolayers, but not to the domains of the *trans S*−Cu−*R*′ monolayers. By symmetry, the same principal holds for the monolayers and water soluble copper complexes of α-amino acids of the opposite handedness.

Introduction

The ability to monitor structural organization of chiral molecules during the early stages of crystal nucleation is of importance in pure and applied sciences.

Clusters formed in supersaturated solutions had been shown to play a ubiquitous role in crystallization processes. Recently, we proposed that among structured clusters there are those that resemble the structure of the macroscopic three-dimensional (3-D) crystalline phase. By applying this working hypothesis, it became possible to design auxiliary molecules that can be stereospecifically and enantioselectively targeted at the surfaces of some of these clusters and inhibit their growth.[1] This methodology was successfully applied for the control of crystal polymorphism,[2−4] inducing[5,6] and preventing[7] crystal twinning and the optical resolution of enantiomers by kinetic crystallization.[8,9]

Several years ago, Harada et al.[10] demonstrated that crystallization of copper complexes of racemic aspartic acid in the presence of the optically pure α-amino acid, e.g., (*S*)-glutamic acid, results in the precipitation of crystalline copper (*R*,*R*)-aspartate. To explain this induction, we proposed that the copper complexes of (*S*)-glutamic acid interact enantioselectively and inhibit the nucleation of the clusters of *S*-aspartate and prevent their conversion to the 3-D crystals[11] (Scheme 1). This mechanism appears to be of general applicability, as demonstrated for a large number of systems.[12]

SCHEME 1

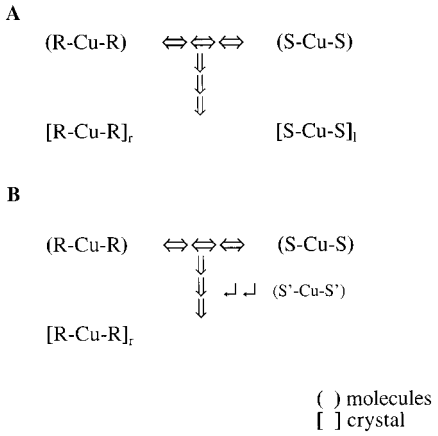

One way to obtain information on interactions between clusters and chiral molecules is by studies on the oriented growth of crystals at the air−solution interface induced by amphiphilic chiral-resolved molecules. For example, crystals of the centrosymmetric α-form of glycine, grown underneath a Langmuir film of an optically pure water-insoluble α-amino acid, were found to be attached to the monolayer via one of the two enantiotopic (010) or ($0\bar{1}0$) faces, depending on the absolute configuration of the monolayer molecules.[13,14] Such observations

[†] The Weizmann Institute of Science.
[‡] Risø National Laboratory.
[§] H. C. Ørsted Laboratory.

10.1021/jp990561g CCC: $18.00
Published on Web 07/29/1999

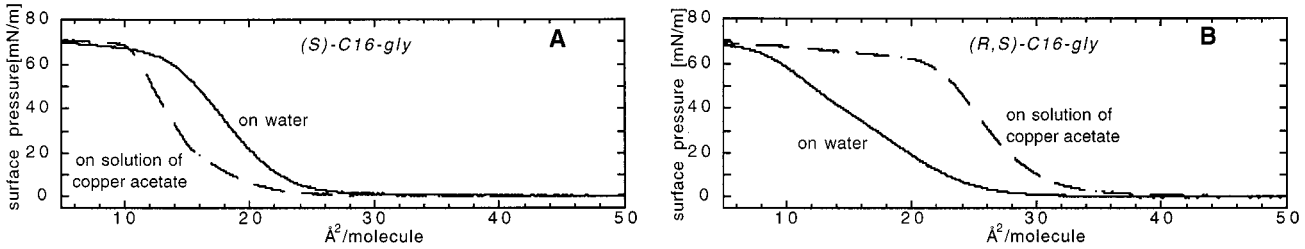

Figure 1. Surface pressure−molecular area isotherms of C_{16}-gly on pure water (solid line) and copper acetate (broken line) solution: (A) chiral resolved (*S*)-C_{16}-gly; (B) racemic (*R*,*S*)-C_{16}-gly.

led to the conclusion that the water-insoluble α-amino acids at the air−solution interface spontaneously form crystalline domains whose polar headgroups serve as a template for an "epitaxial" nucleation of 3-D crystals.

Here we present studies on the interactions between the amphiphilic diastereomeric copper−α-amino acid complexes at the air−solution interface and water-soluble complexes of the environment. We made use of Cu^{2+} ions since they can bind both with a glycine headgroup of the amphiphile and water-soluble α-amino acid[15] molecule from the aqueous subphase. Langmuir films of optically resolved *S* or *R* and racemic (*R*,*S*) α-amino acids $C_{16}H_{33}-CH(NH_3^+)-COO^-$ (C_{16}-gly) and $C_{15}H_{31}-CONH-(CH_2)_4-CH(NH_3^+)-COO^-$ (C_{15}-lys) were investigated on pure copper acetate solution and in the presence of the optically resolved (*S*)- or (*R*)-alanine, -serine, and -valine (hereafter labeled *R*′ or *S*′). The structures of the thin films at the air−solution interface were studied by surface pressure vs molecular area ($\pi-A$) isotherms and grazing-incidence X-ray diffraction (GIXD) and by scanning force microscopy (SFM) and X-ray photoelectron spectroscopy (XPS) after deposition onto a solid support.

Experimental Section

Materials. The compounds used in this study are (*S*)- and (*R*,*S*)-α-aminostearic acid, prepared according to a known procedure,[16] and palmitoyl-*N*$^{\epsilon}$-lysine ($C_{15}H_{31}-CO^{\epsilon}NH-(CH_2)_4-CH(NH_3^+)CO_2-$) as the α-amino acids bearing an amide functional group within the chain. The racemic and optically pure long-chain α-amino acids have been synthesized and their purity assessed according to procedures described previously.[17] Serine, valine, alanine, and copper acetate were purchased from Sigma and used with no further purification.

$\pi-A$ Isotherms. The surface pressure−molecular area isotherms of the films of enantiomerically pure and racemic amphiphiles were measured on an automatic Lauda film balance on both pure water and copper acetate solution ($c = 10^{-3}$ M). Enantiomerically pure and racemic aqueous solutions of serine, valine, and alanine were injected after monolayer formation on the surface of copper acetate solution. The concentration and amount of the α-amino acid solutions were calculated for a 100 times excess over the concentration of Cu^{2+} ions.

GIXD Experiments. The films on liquid surfaces for the grazing incidence X-ray diffraction experiments were prepared by spreading ∼0.5 mM solutions of the amphiphiles in a 98:2 mixture of chloroform−trifluoroacetic acid. The films were compressed to nominal areas per molecule 36 and 25 Å^2 and cooled to 5 °C. For both nominal areas per molecule the surface pressure was essentially zero.

GIXD experiments were performed on the liquid-surface diffractometer at beam line BW1 at HASYLAB, DESY, Hamburg. The dimensions of the footprint of the incoming X-ray beam on the liquid surface were approximately 5 × 50 mm^2. The scattered intensity was collected by means of a vertical position-sensitive detector (PSD), which intercepts photons over the range $0 \le q_z \le 0.9$ Å^{-1} (q_z is the vertical component of the X-ray scattering vector). Measurements were performed by scanning the horizontal component of the scattering vector, q_{xy}, and simultaneously resolving q_z with the PSD. Diffraction data are represented in three ways: (1) as contour plots $I(q_{xy},q_z)$; (2) Bragg peak intensity profiles $I(q_{xy})$ obtained by integrating the whole q_z intensity for any q_{xy} along the measured range; (3) Bragg rod profiles $I(q_z)$ in channels along the PSD, integrated over the whole range in q_{xy} for a Bragg peak. The q_{xy} positions of the Bragg peaks yield the lattice repeat distance $d = 2\pi/q_{xy}$, which may be indexed by the two Miller indices *h* and *k* to yield the unit cell. The full width at half-maximum (fwhm) of the Bragg peaks in q_{xy} units yields the 2D crystalline coherence length associated with the *h*,*k* reflection. The width Δq_z of the Bragg rod profile along q_z gives a measure of the thickness of the crystalline film, $T \approx 0.9(2\pi)/\Delta q_z$. More detailed descriptions of the GIXD method used for monolayer structure determination are given in the refs 18−20.

X-ray Powder Diffraction. Crystals of racemic and chiral-resolved serine copper complexes were grown from water−ethanol mixtures. X-ray powder diffraction spectra (40 kV, 120 mA) of the grown crystals obtained on a Rigaku Rotaflex RU-200B diffractometer were in agreement with the reported single-crystal structures.[21,22]

XPS Studies. X-ray photoelectron spectroscopy spectra were obtained by using a Kratos AXIS-HS spectrometer with a monochromatic Al (Kα) radiation source (1486.6 eV). The shift of the spectral lines due to the effect of charging was compensated by a flood gun, while a fine correction for the energy scale calibration was done with respect to the substrate Si 2p3/2 line at 103.3 eV. The experimental precision of energy line positions is ∼0.025 eV, much beyond the instrumental energy resolution. This fact could be used by carefully comparing the full line shapes, making use of the fit obtained by a large (∼100) number of data points. To avoid observable damage of the samples, each scan was performed on a fresh spot, such that the overall exposure was kept minimal; the statistical signal-to-noise ratio for the weakest lines was 4−4.5. The samples were prepared by depositing the floating films of amphiphilic complexes on a glass support by the Langmuir−Blodgett technique using a Nima (NIMA Technology, Coventry, U.K.) trough at target pressure 25 mN/Å^2 and room temperature. The typical transfer ratios were 85−90%.

SFM Studies. A scanning force microscope (Nanoscope III, Digital Instruments) in a contact mode was used to image the films transferred on atomically smooth mica. The floating monolayer films were transferred onto freshly cleaved mica pieces (1 × 1 cm) in a specially constructed Teflon trough (surface area 20 cm^2) by draining the subphase solution with a motor-driven syringe. The calculated surface coverage was equal to 90%, assuming the formation of a monomolecular film.

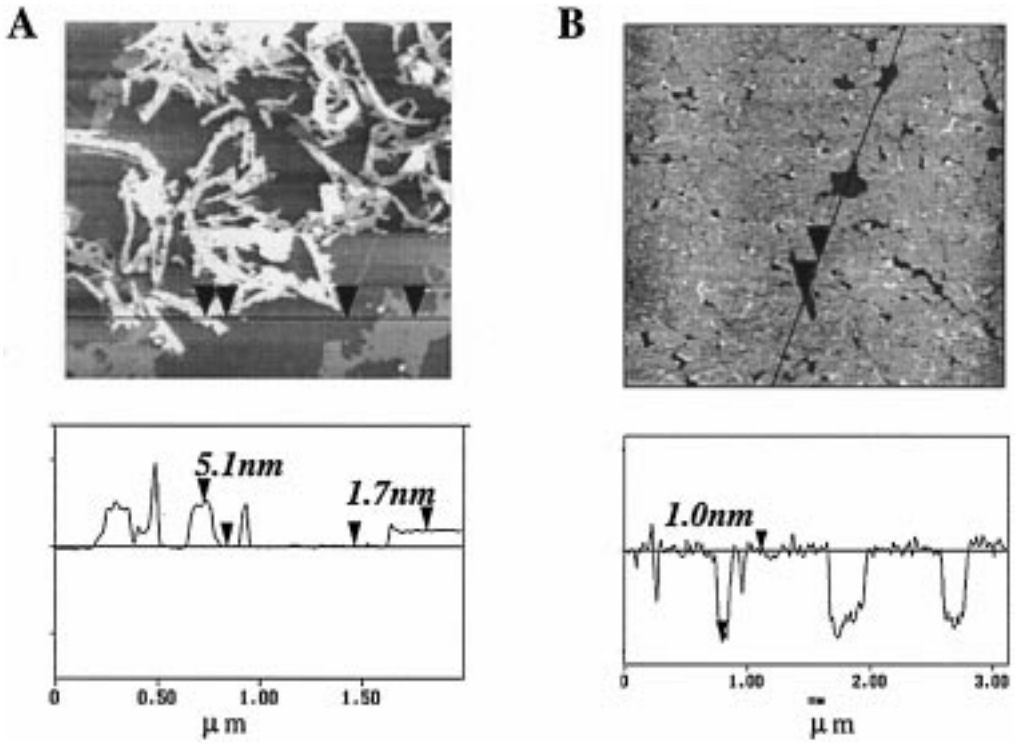

Figure 2. Scanning force microscopy images of chiral-resolved (A) and racemic (B) C_{16}-gly after transfer from a copper acetate subphase onto atomically smooth mica.

TABLE 1: Crystallographic Data for the Monolayers

parameters	(*R*,*S*)-C_{16}-gly	(*S*)-C_{16}-gly	(*R*,*S*)-C_{15}-gly	(*S*)-C_{15}-gly	*S*−Cu−*S*′	*S*−Cu−*R*′
lattice spacings[a] (Å)	subcell	subcell		subcell		
d_{10}		4.72	4.59	4.69	4.74	4.88
d_{01}		4.72		6.22	5.02	4.95
$d_{1\bar{1}}$	4.99	4.41				3.76
d_{11}	4.72			4.21	3.20	3.20
d_{02}	4.01					
av FWHM[b] (Å^{-1})	0.176	0.235	1.402	0.160	0.857	1.233
av coherence length[c] (Å)	230	170	30	255	45	35
a (Å)	6.10	5.22		4.80	4.80	4.93
b (Å)	4.97	5.22		6.39	5.09	5.01
γ (deg)	54.1	64.7		77.4	99.0	98.5
tilt angle (deg)	34	37		50		
unit cell area (Å^2)	24.6	24.6		29.9	24.2	24.4
chain cross-sectional area (Å^2)	20.4	20.6		19		

[a] Lattice spacings are given according to the indexing. [b] FWHM, full width at half-maximum of the Bragg peak in q_{xy} units. [c] The coherence length *L* has been calculated using the standard Sherrer equation:[33] $L = (0.9 \times 2\pi)/(\mathrm{FWHM}^2 - \Delta^2)^{1/2}$, where the resolution of the Soller collimator, $\Delta = 0.0081$ Å^{-1} (in q_{xy} units).

Results and Discussion

Assembly of Amphiphilic α-Amino Acids on Copper Acetate Solution. α-*Amino Alkanoic Acid.* The formation and the structure of stable monolayers of both optically resolved (*S*)- and racemic (*R*,*S*)-α-aminostearic acid (C_{16}-gly) on water were reported recently.[14] On a copper acetate solution the monolayer of (*S*)-C_{16}-gly displayed a $\pi-A$ isotherm with a limiting surface area of 18 Å^2, compared to 25 Å^2 on pure water (Figure 1a). The racemate behaves differently, with a limiting area of 34 Å^2 on copper acetate (Figure 1b). After a transfer onto atomically smooth mica, the films were examined by SFM (Figure 2). Such a measurement of (*S*)-C_{16}-gly yielded two typical heights of 17 and 51 Å; the film of (*R*,*S*)-C_{16}-gly, on the other hand, had an average thickness of 9−10 Å.

The films of chiral (*S*)- and (*R*,*S*)-C_{16}-gly on copper acetate solution were studied by GIXD. The (*S*) and (*R*,*S*) systems gave rise to two different diffraction patterns that did not change upon compression from 36 to 25 Å^2 per molecule. The average fwhm of the strongest Bragg peaks and corresponding coherence lengths are given in Table 1. These GIXD patterns were different from those observed on pure water,[14] therefore suggesting binding of Cu ions to the amphiphilic molecules.

The GIXD pattern of (*R*,*S*)-C_{16}-gly on copper acetate solution was indexed in terms of a pseudorectangular cell, $a = 6.10$ Å, $b = 8.06$ Å, $\gamma = 92.01°$, $A = 49.2$ Å^2, consistent with two symmetry-independent amphiphilic molecules in the unit cell (Figure 3a). The Bragg rod of each of the three reflections (1,1), (1,$\bar{1}$) and (0,2) has one strong intensity modulation with a full width at half-maximum (fwhm) = 0.32 Å^{-1}, corresponding to a monolayer 19.6 Å thick. By contrast, the Bragg rods of the low order (1,0) and (0,1) reflections demonstrate modulations with a fwhm $\sim$ 0.15 Å^{-1} (Figure 3c,*i*). We can attribute the presence of these sharp modulations to a difference in the height of the two symmetry-independent long-chain molecules due to the complexation with Cu^{2+} ions. The modulations of about the same frequency but of a lower amplitude are present for a

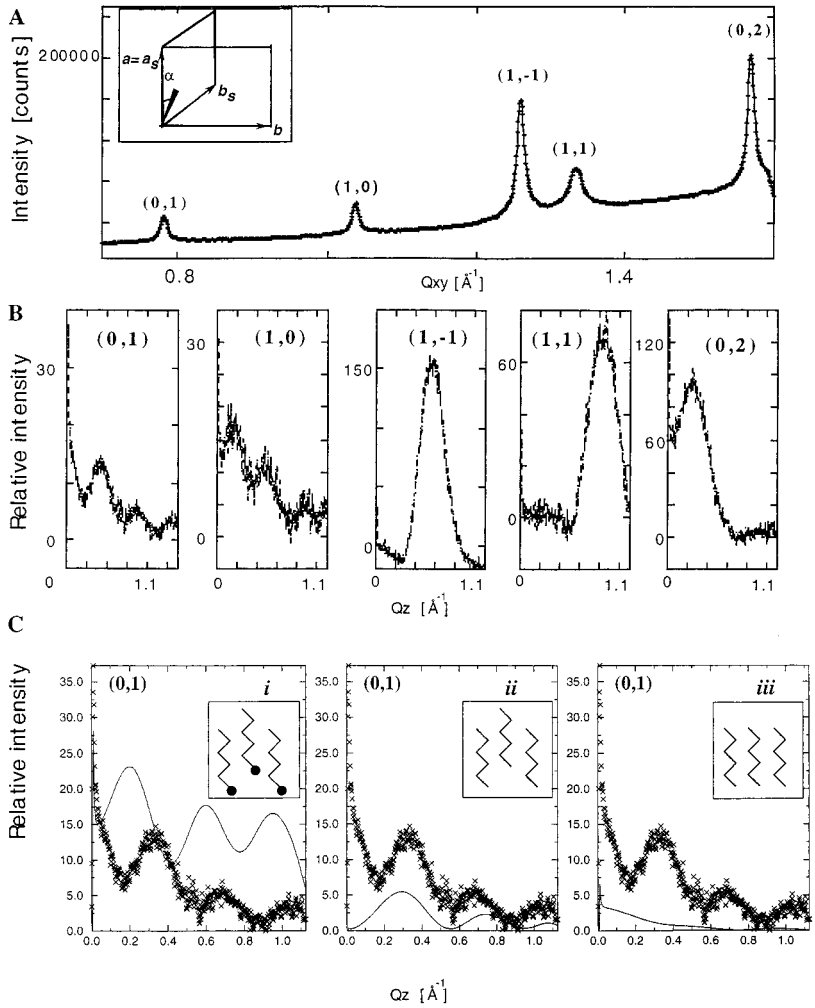

Figure 3. Grazing incidence X-ray diffraction pattern of racemic C_{16}-gly spread on a copper acetate solution. (A) Bragg peaks with the assigned (*h*,*k*) indices. The inset shows the two-dimensional unit cell and the subcell corresponding to the hydrocarbon chain packing. The angle between the projection of the tilted chain (indicated as a wedge) onto the *ab* plane and the *a* axis is $\alpha = 15°$. (B) Bragg rods corresponding to the measured Bragg peaks shown in (A). (C) Observed (×) and calculated (—) (0,1) Bragg rod with two independent molecules at the unit cell and 4 Å separation along the *z* direction between them ($\Delta z \sim 2.5$ Å): (*i*) corresponds to the model of the racemic α-aminostearic acid with Cu^{2+} ions bound to it; (*ii*) corresponds to the simplified model of the monolayer molecules without contribution of the headgroups ($\Delta z \sim 2.5$ Å); (*iii*) corresponds to two hydrocarbon chains at the same level ($\Delta z = 0$). The insets show the simplified monolayer structures used for Bragg rod calculation.

simplified model that only involves the hydrocarbon chains with 2.5 Å shift in height (Figure 3c,*ii*). As expected, the modulations vanish when the two hydrocarbon chains are positioned at the same level ($\Delta z = 0$) as depicted in Figure 3c,*iii*. Therefore, we interpret the strong reflections (1,1), (1,$\bar{1}$) and (0,2) as arising primarily[23] from the hydrocarbon chains in a subcell $a_s = a = 6.10$ Å, $b_s = (a + b)/2 = 4.97$ Å, $\gamma_s = 54.1°$, $A_s = 24.6$ Å^2 (Figure 3a, inset).

The tilt of the hydrocarbon chains was calculated from the q_z positions of the maxima of the (1,1), (1,$\bar{1}$) and (0,2) Bragg rods. The aliphatic chains, in the film of 19.6 Å thickness, are tilted at an angle of 34° from the normal to the *ab* plane, which corresponds to a chain length of about 19.6/cos 34° = 24 Å, a value consistent with the length of a $C_{16}H_{33}$ chain. The direction of the tilted chain projected onto the *ab* plane is shown in Figure 3a (inset); the cross-sectional area occupied by such a chain is about $A_s \cos 34° = 20.4$ Å^2.

On the basis of the above GIXD data we could not conclude whether a spontaneous separation of enantiomers had taken place or not, since the two crystallographically independent molecules in the unit cell might be of the same or of opposite handedness. This question was resolved by making use of optically resolved (*S*)-C_{16}-gly.

The (*S*)-C_{16}-gly spread over the copper acetate solution displayed a GIXD pattern (Figure 4a) different from that of (*R*,*S*)-C_{16}-gly, indicating that the latter film is not phase-separated into domains of opposite handedness but rather heterochiral. All the twelve observed Bragg peaks of (*S*)-C_{16}-gly (Figure 4a) were indexed according to an oblique unit cell of dimension $a = 15.65$ Å, $b = 14.63$ Å, $\gamma = 104.7°$, $A = 221.54$ Å^2. The Bragg rods of the strong (3,1) and coinciding (0,3) and (3,$\bar{2}$) reflections (Figure 4b) have fwhm (q_z) = 0.33 Å^{-1}, corresponding to a monolayer ~19 Å thick, as in the racemic system. These three reflections (Figure 4a) correspond to a subcell of hydrocarbon chain packing $a_s = a/3 = 5.22$ Å, $b_s = (2a/3 + b)/3 = 5.22$ Å, $\gamma_s = 64.7°$, $A_s = 24.6$ Å^2, $A{:}A_s$ = 9:1. The relationship between the subcell (a_s, b_s) and the unit cell (*a*, *b*) is given in Figure 4a (inset). The intensity maxima of the (3,1) and partially resolved (0,3) and (3,$\bar{2}$) Bragg rod profiles yielded a chain tilt of 37°, and a resulting cross-sectional area of $A_s \cos 37° = 20.6$ Å^2. The chains are tilted in a direction almost perpendicular to the diagonal ($a + b$), as shown in Figure 4a (inset). The Bragg rod of the weak (0,1) reflection is modulated (Figure 4c) similar to the (0,1) and (1,0) Bragg rods of the (*R*,*S*)-C_{16}-gly-Cu diffraction pattern (Figure 3b).[24]

The fwhm (=0.33 Å^{-1}) of the Bragg rod modulation of the

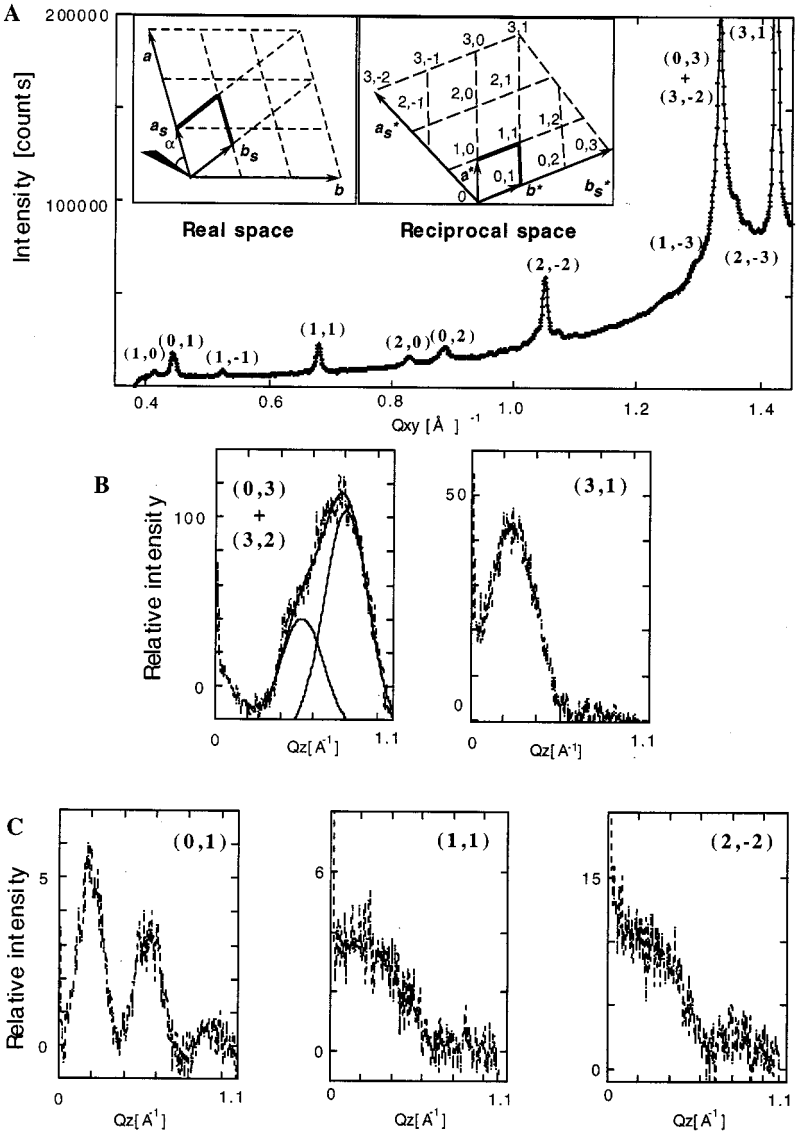

Figure 4. Grazing incidence diffraction pattern of chiral-resolved C_{16}-gly spread over a copper acetate solution. (A) Bragg peaks with the assigned (*h*,*k*) indices. The inset shows the two-dimensional unit cell, and the subcell corresponding to the hydrocarbon chain packing, in real and reciprocal space. The angle between the projection of the tilted chain (indicated as a wedge) onto the *ab* plane and the *a* axis is $\alpha = 50°$. (B) Bragg rods of those reflections with a major contribution from the hydrocarbon chains. (C) Bragg rods of those reflections with a major contribution from the headgroups.

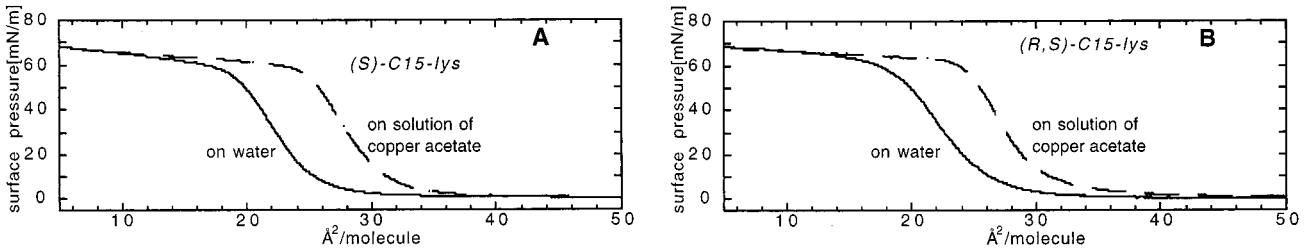

Figure 5. Surface pressure−area isotherms of chiral resolved (A) and racemic (B) C_{15}-lys on water (solid line) and on copper acetate (broken line) solutions.

(0,3), (3,$\bar{2}$), and (3,1) reflections corresponding to the hydrocarbon chain packing (subcell) unambiguously indicate that (*S*)-C_{16}-gly forms a crystalline monolayer on the $Cu(Ac)_2$ subphase with the thickness of the film equal to 19 Å. However, the low surface area per molecule obtained by isotherm measurements as well as the results of SFM experiments suggest partial multilayer formation. We therefore conclude that the multilayers formed at the air−liquid interface are not crystalline and do not contribute to the diffraction pattern.

α-Amino Acid Amphiphile Bearing an Amide Group in the Chain. As discussed above, we made use of an amide group in the hydrocarbon chain in order to achieve a spontaneous separation of enantiomers in a Langmuir monolayer of the α-amino acids on pure water.[14]

The isotherms of chiral-resolved and racemic C_{15}-lys on an aqueous solution of copper acetate ($c = 10^{-3}$ M) (Figure 5a,b, curve 2) are more expanded than on pure water (Figure 5a,b curve 1), indicating that the Cu ions from the subphase interact

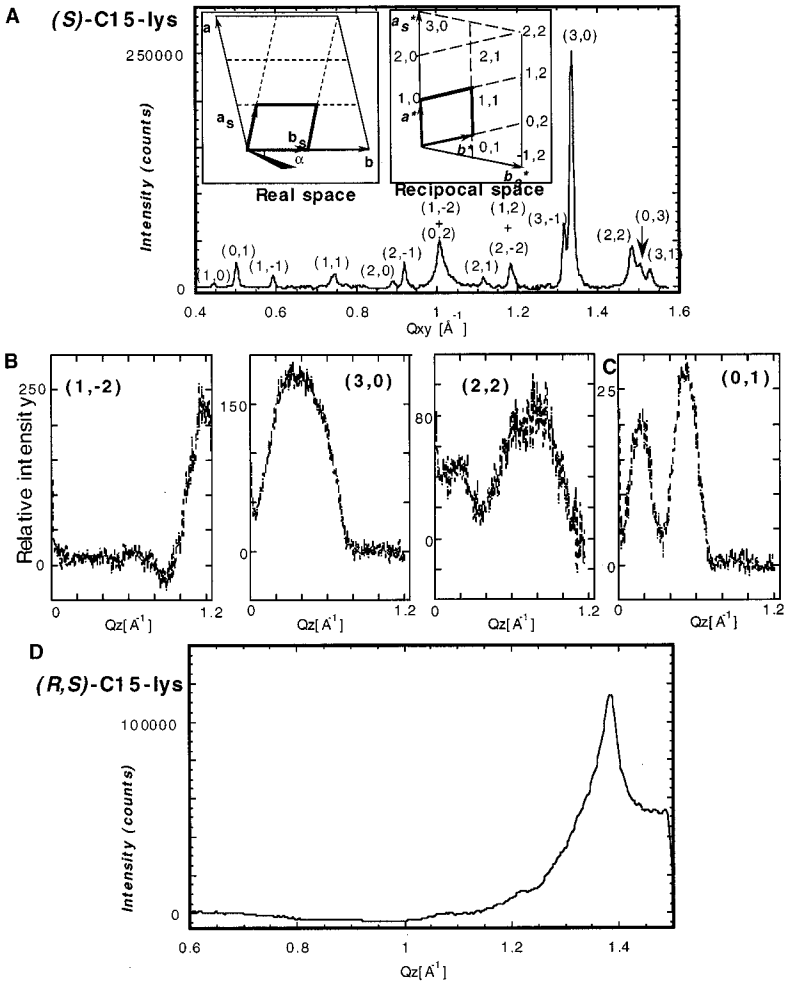

Figure 6. Grazing incidence diffraction pattern of chiral-resolved C_{15}-lys spread over copper acetate solution. (A) Bragg peaks with the assigned (*h*,*k*) indices. The inset shows the two-dimensional unit cell, and the subcell corresponding to the hydrocarbon chain packing, in real and reciprocal space. Angle $\alpha = 12°$ is between the projection of the tilted chain (indicated as a wedge) onto the *ab* plane and the *b* axis. (B) Bragg rods of those reflections with a major contribution from the hydrocarbon chains. (C) Intensity modulations along the Bragg rod of the (0,1) reflection shown in (A). (D) Bragg peak of (*R*,*S*)-C_{15}-lys.

with the headgroups of the amphiphile. Neither dilution of the copper acetate solution down to 10^{-5} M nor variation of the subphase temperature from 5 to 28 °C caused any noticeable change in the isotherm behavior.

The interaction between the monolayer and copper ions was also confirmed by the substantial differences in the GIXD patterns of the chiral resolved and racemic C_{15}-lys on the copper acetate solution (Figure 6, Table 1) and on pure water.[14]

The GIXD pattern of (*R*,*S*)-C_{15}-lys on the $Cu(Ac)_2$ solution is depicted in Figure 6d. One very broad strong Bragg peak (Table 1) arising from the hydrocarbon chain packing was observed, indicating that the racemic monolayer is poorly ordered.

The (*S*)-C_{15}-lys on copper acetate solution displayed a GIXD pattern (Figure 6a) with 14 narrow reflections. All the measured Bragg peaks were indexed in terms of a large oblique unit cell of dimensions $a = 14.40$ Å, $b = 12.77$ Å, $\gamma = 103.0°$, and $A = 179.2$ Å^2. The three strong reflections $(1,\bar{2})$, (3,0), (2,2) correspond to a subcell of hydrocarbon chain packing $a_s = (a + b/2)/3 = 4.80$ Å, $b_s = b/2 = 6.39$ Å, $\gamma_s = 77.4°$, $A_s = 29.9$ Å^2 (A:A_s = 6:1), indicating that the supercell (*a*, *b*), as shown in Figure 6a (inset), contains six amphiphilic molecules. The hydrocarbon chains are tilted by 50° from the layer normal in the direction of the $b_s - a_s$ vector (see Figure 6a, inset), as calculated from positions of the intensity profile maxima of $(1,\bar{2})$, (3,0), and (2,2) Bragg rods. The resulting cross-sectional area per chain is $A_s \cos 50° = 19$ Å^2 that complies with the published data of hydrocarbon chains in two-dimensional crystals.[19] The average fwhm of the Bragg rod intensity profiles of (3,0) and (2,2) reflections is 0.45 Å^{-1}, which corresponds to a film thickness of ~14 Å. We rationalize the observed intensity modulations of the low order reflections, such as of the (0,1) reflection (Figure 6c), as arising from the contribution of symmetry-independent molecules with different *z*-coordinates.

We may conclude that the enantiomers in the racemic film do not separate into islands of opposite handedness, as it was observed for such molecules on pure water.[14]

We conclude that racemic α-amino acids containing either a regular hydrocarbon chain or one with an amide linkage do not separate into domains of opposite handedness at the air−copper acetate solution interface and that the racemic films are less crystalline than chiral-resolved ones. The lack of chiral segregation may arise from constraints imposed by the effect of copper complexation on the conformation of the headgroup, which precludes formation of a two-dimensional net of N− H···O hydrogen bonds.

Chiral Discrimination of C_{15}-lys on Copper Solutions of Water-Soluble α-Amino Acids. Here we examine the diastereomeric interactions between the monolayers of chiral-resolved (*S*)-C_{15}-lys on copper acetate solutions with optically pure (*R*′

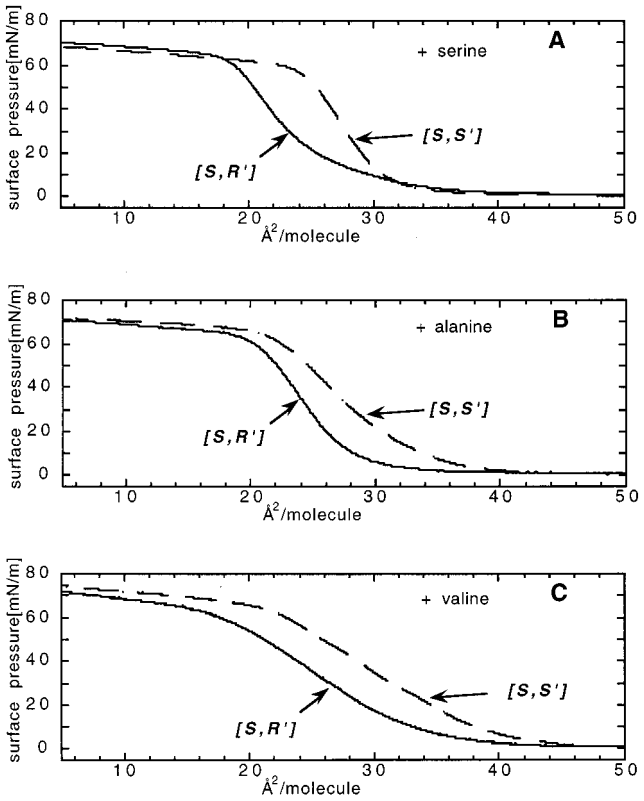

Figure 7. Effect on the surface pressure−area isotherms of (*S*)-C_{15}-lys of injecting of (A) serine, (B) alanine, and (C) valine into the copper acetate solution. [*S*,*S*′], [*S*,*R*′] refer to isotherm of the (*S*) amphiphile on the subphase containing the injected (*S*′) or (*R*′) water-soluble α-amino acid, respectively.

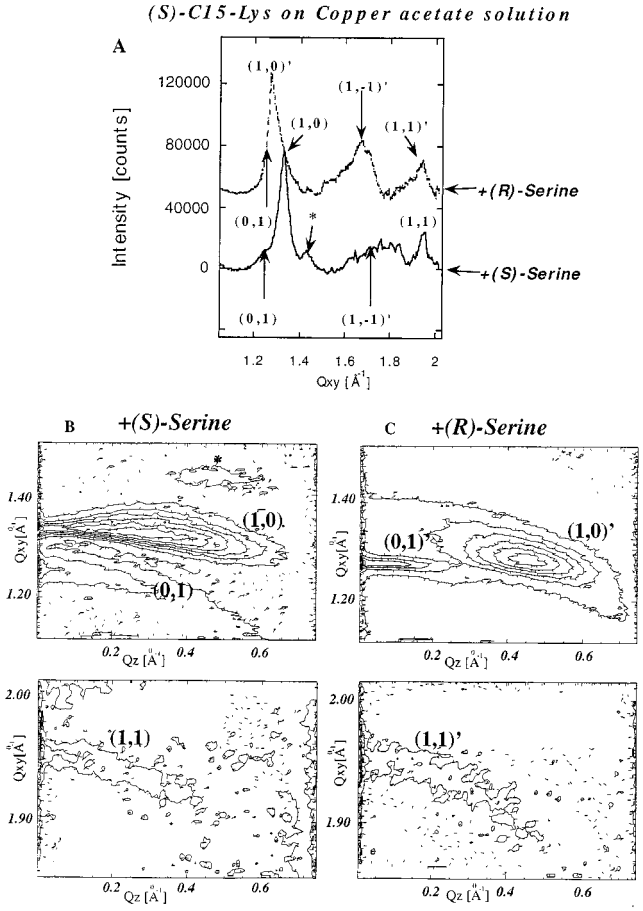

Figure 8. Grazing incidence diffraction pattern of (*S*)-C_{15}-lys spread over a copper acetate solution followed by injection of *S*-serine and *R*-serine. Bragg peaks (upper part) and two-dimensional intensity contour plots $I(q_{xy},q_z)$ (lower part). The Bragg rods of the (1,−1) and (1,−1)′ reflections were not measured.

or *S*′) alanine, serine, or valine injected into the subphase. The possibility of artifacts caused by impurities was ruled out by cross-check experiments involving the use of amphiphilic and water-soluble α-amino acids of both handedness.

Injection of the water-soluble component with an absolute configuration the same (i.e., *S*′) as that of the amphiphile (i.e., *S*) led to a more expanded pressure−area isotherm than for the two chiral components of opposite handedness (i.e., *S*,*R*′) (Figure 7). Injection of valine led to more expanded isotherms than the use of either serine or alanine (cf. Figure 7c and Figure 7a,b).

Injection of either (*R*′)- or (*S*′)-serine into the copper acetate subphase under the enantiomeric (*S*)-C_{15}-lys monolayer induced a change in the GIXD pattern (cf. Figures 6 and 8). The supercell reflections arising from the contribution of the copper ions disappeared. Three distinct reflections were observed for each of the two diastereomeric systems (*S*−Cu−*S*′) and (*S*−Cu−*R*′) (Figure 8). Each diffraction pattern was indexed in terms of an oblique unit cell of dimensions $a = 4.93$ Å, $b = 5.01$ Å, $\gamma = 98.5°$, $A = 24.4$ Å^2 for (*S*,*R*′) and $a = 4.80$ Å, $b = 5.09$ Å, $\gamma = 99.0°$, $A_s = 24.2$ Å^2 for (*S*,*S*′) monolayers. In the diffraction pattern of the (*S*−Cu−*S*′) monolayer, one weak reflection observed at $q_{xy} = 1.44$ Å^{-1} (labeled *) could not be indexed and probably arises from a minor crystalline phase.

Noticeable differences in the diffraction patterns of the (*S*−Cu−*S*′) and (*S*−Cu−*R*′) films indicate somewhat dissimilar molecular packing arrangements of the two diastereomeric systems. These GIXD results are compatible with ordered binding of the water-soluble α-amino acids to the headgroups of the amphiphiles via copper ion complexation. These measurements, however, cannot explain the observed variation of the surface pressure−area isotherms (Figure 7).

Some of the copper complexes of optically pure α-amino

SCHEME 2

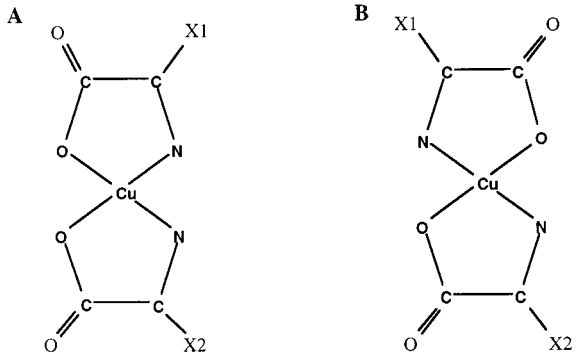

X1- HOCH2- or C15H31-CONH-(CH2)4-

X2- HOCH2-

acids (Cu*S*′$_2$) adopt in bulk crystals a *cis*-configuration (Scheme 2a), whereas their racemic analogues (Cu*S*′*R*′) are usually in the *trans* form.[21,22,25−28] (Scheme 2b). The racemic complex of serine,[21] which lies on a crystallographical inversion center and is centrosymmetric, thus has a *trans* configuration (Scheme 2b), while the Cu(*S*′-ser)$_2$ complex[22] (Scheme 2a) exhibits a local 2-fold symmetry with a *cis* arrangement of the two serine residues about the Cu atom. In the XPS measurements of these 3-D crystalline complexes, the binding energy line of Cu(2p) of the *trans* copper complex of racemic serine is 0.23(5) eV

TABLE 2: Chemical Shift of the Elements of the Film Deposited on a Glass Support[a]

system	copper	carbon from the hydrocarbon chain	nitrogen from the amide group of the hydrocarbon chain
$S-Cu-R'$	934.95 ± 0.02	285.98 ± 0.02	399.89 ± 0.01
$S-Cu-S'$	934.70 ± 0.02	285.99 ± 0.02	399.88 ± 0.01
$R-Cu-R'$	934.72 ± 0.02	284.98 ± 0.02	399.89 ± 0.01

[a] The binding energy line positions are given in electronvolts. The given errors and binding energy values are obtained by statistical averaging over repeated measurements.

higher than that of the *cis* copper complex of the chiral-resolved serine. Comparative XPS measurements of 3-D crystals of the copper complexes $S'-Cu-S'$ and S'-Cu-R' and the 2-D films of $S-Cu-S'$ and $S-Cu-R'$ (where S' and R' are serine and S is C15-lys residues) transferred from the liquid interface onto a solid support shed light on the variation of the headgroup structure of the two amphiphilic complexes. The relative atomic concentration of [Cu] to [N] deduced from the XPS measurements of the 2-D films is in agreement with formation of $S-Cu-S'$ and $S-Cu-R'$ complexes. The binding energies of C and N atoms constituting the chain of the two diastereomeric complexes are essentially identical, whereas distinct differences in binding energies for the Cu ions were observed (Table 2). The binding energy line of Cu(2p) for the $S-Cu-R'$ complex is approximately 0.24 eV higher than that of the $S-Cu-S'$ (or $R-Cu-R'$) complex.[29] This value is almost equal to the corresponding difference obtained from the 3-D crystals of Cu complexes of serine. This match indicates a structural similarity between the complexes of Cu(S'-ser)$_2$ and Cu(S'-ser)(R'-ser) in the bulk crystals and the corresponding $S-Cu-S'$ and $S-Cu-R'$ thin films.[30,31] Therefore we propose that the α-amino acid groups in the amphiphilic complex $S-Cu-S'$ appears in the *cis* form, whereas the complex $S-Cu-R'$ appears in the *trans* form (Scheme 2).

Concluding Remarks

We rationalize the differences in the isotherm behavior of $S-Cu-S'$ and $S-Cu-R'$ complexes in terms of the GIXD data, the XPS measurements, and molecular packing considerations. First we note that the 2-D crystal structures of the $S-Cu-S'$ and $S-Cu-R'$ complexes are different according to the GIXD data and by the XPS measurements. We propose the following molecular packing of the $S-Cu-S'$ and $S-Cu-R'$ complexes based on 3-D crystal structures of the Cu complexes and hydrogen bonding between amphiphilic chains via N− H···O bonds (Figure 9).

We propose that the homochiral water-soluble $S'-Cu-S'$ (or $R'-Cu-R'$) complexes existing in the subphase should be attached to the periphery of the $S-Cu-S'$ (or $R-Cu-R'$) crystalline monolayer islands (Scheme 3) more strongly than to the islands of $R-Cu-S'$ (or $S-Cu-R'$) by virtue of a better molecular fit. This preferred and stereoselective attachment leads to a larger effective domain size of the $S-Cu-S'$ complex (cf. Scheme 3a and b) and thus to a more expanded isotherm. A similar type of interaction between 2-D crystallites with water-soluble molecules was deduced from inhibition of growth of 2-D crystals of perfluorododecyl−aspartate in the presence of glycine in the aqueous subphase and of the complete destruction of 2-D crystallinity with β-alanine in solution.[19]

This process of diastereoselective attachment of water-soluble copper complexes should be akin to the attachment of "tailor-made" auxiliary molecules to the surfaces of growing three-dimensional nuclei or crystals.[12,32] The present observations provide insight into the stereospecific interactions between small clusters and molecules of the environment, and their resulting structure.

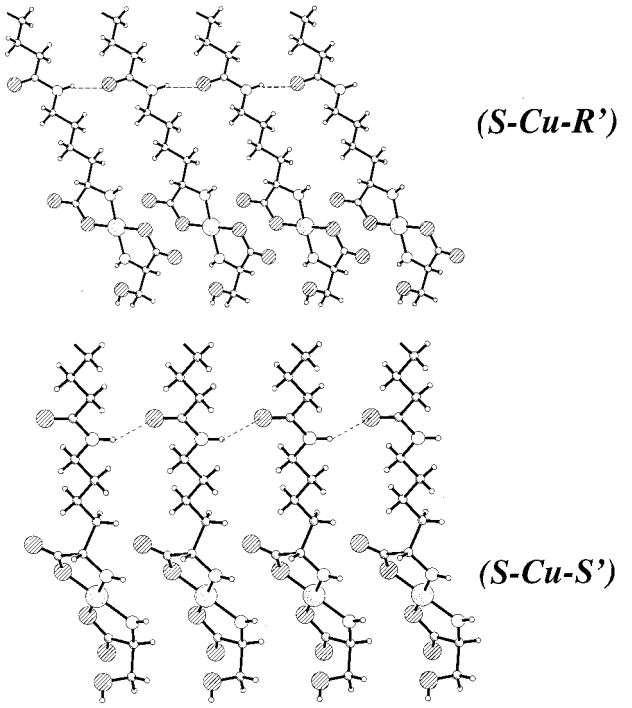

Figure 9. Plausible monolayer packing arrangements of the two amphiphilic diastereomeric copper complexes: the amphiphilic ligand is (S)-C_{15}-lys; the water-soluble α-amino acid is (top) (R')-serine and (bottom) (S')-serine.

SCHEME 3

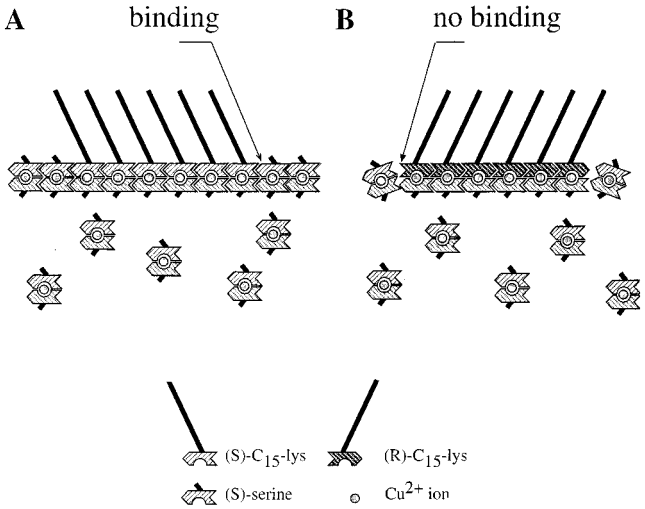

Acknowledgment. We thank Dr. S. Mathlis for the SFM and R. Buller for some of the surface pressure vs molecular area isotherm measurements. We acknowledge financial support from the German Israeli Foundation, GIF, and the Dansyne program of the Danish Foundation for Natural Sciences and E.U.'s TMR program, and we thank HASYLAB, Desy, Hamburg, for synchrotron beam time.

References and Notes

(1) Weissbuch, I.; Addadi, L.; Leiserowitz, L.; Lahav, M. *Science* **1991**, *253*, 637.

(2) Weissbuch, I.; Zbaida, D.; Addadi, L.; Leiserowitz, L.; Lahav, M. *J. Am. Chem. Soc.* **1987**, *109*, 1869.

(3) Weissbuch, I.; Leiserowitz, L.; Lahav, M. *Adv. Mater.* **1994**, *6*, 952.
(4) Staab, E.; Addadi, L.; Leiserowitz, L.; Lahav, M. *Adv. Mater.* **1990**, *2*, 40.
(5) Weissbuch, I.; Kuzmenko, I.; Vaida, M.; Zait, S.; Leiserowitz, L.; Lahav, M. *Chem. Mater.* **1994**, *6*, 1258.
(6) Edgar, R.; Schultz, T. M.; Rasmussen, F. B.; Feidenhans'l, R.; Leiserowitz, L. *J. Am. Chem. Soc.* **1999**, *121*, 632.
(7) Berfeld, M.; Zbaida, D.; Leiserowitz, L.; Lahav, M. *Adv. Mater.* **1999**, *11*, 328.
(8) Addadi, L.; Weinstein, S.; Gati, E.; Weissbuch, I.; Lahav, M. *J. Am. Chem. Soc.* **1982**, *104*, 4610.
(9) Addadi, L.; Van Mil, J.; Lahav, M. *J. Am. Chem. Soc.* **1982**, *104*, 3422.
(10) Harada, K. *Nature* **1965**, *205*, 590.
(11) Addadi, L.; Van Mil, J.; Lahav, M. *J. Am. Chem. Soc.* **1981**, *103*, 1249.
(12) Addadi, L.; Berkovitch-Yellin, Z.; Weissbuch, I.; Van Mil, J.; Shimon, L. J. W.; Lahav, M.; Leiserowitz, L. *Angew. Chem., Int. Ed. Engl.* **1985**, *24*, 466.
(13) Weissbuch, I.; Addadi, L.; Bercovitch-Yellin, Z.; Gati, E.; Lahav, M.; Leiserowitz, L. *Nature* **1984**, *310*, 161.
(14) Weissbuch, I.; Berfeld, M.; Bowman, W.; Kjaer, K.; Als-Nielsen, J.; Lahav, M.; Leiserowitz, L. *J. Am. Chem. Soc.* **1997**, *119*, 933.
(15) Gillard, R. D.; Laurie, S. H. In *Amino acids, Peptides, Proteines. Special Periodical Reports*; Yong, G. T., Ed.; The Chemical Society: London, 1970; Vol. 3, p 323.
(16) Landau, E. M.; Grayer, Wolf, S.; Levanon, M.; Leiserowitz, L.; Lahav, L.; Sagiv, J. *J. Am. Chem. Soc.* **1989**, *111*, 1436.
(17) Paquet, A. *Can. J. Chem.* **1976**, *54*, 733.
(18) Als-Nielsen, J.; Kjaer, K. In *Proceedings of the NATO Advanced Study Institute, Phase Transitions in Soft Condensed Matter*; Riste, T., Sherrington, D., Eds.; Plenum Press: New York,: Geilo, Norway, 1989; p 113.
(19) Als-Nielsen, J.; Jacquemain, D.; Kjaer K.; Leveiller, F.; Lahav, M.; Leiserowitz, L. *Phys. Rep.* **1994**, *246*, 251.
(20) Weissbuch, I.; Popowitz-Biro, R.; Lahav, M.; Leiserowitz, L.; Kjaer, K.; Als-Nielsen, J. In *Advances in Chemical Physics*; Prigogine, I., Rice, S. A., Eds.; John Wiley & Sons: New York, 1997; Vol. 102, p 39.
(21) D'yakon, I. A.; Donu, S. V.; Chapurina, L. F.; Kairyak, L. N. *Sov. Phys. Crystallogr.* **1992**, *37*, 751.
(22) Van Der Helm, D.; Franks, W. A. *Acta Crystallogr.* **1969**, *B25*, 451.
(23) In terms of the monolayer model involving hydrocarbon chains at different heights, we may discard an alternative interpretion of the GIXD pattern incorporating a coexistence of mono- and multilayer.
(24) We cannot account for the fwhm of the (1,1) and (2,−2) reflections which are as broad as 0.65 A^{-1}.
(25) Herlinger, A. W.; Wenhold, S. L.; Long, T. V. *J. Am. Chem. Soc.* **1970**, *92*, 6474.
(26) Steren, C. A.; Calvo, R.; Castellano, E. E.; Fabiane, M. S.; Piro, O. E. *Physica B* **1990**, *164*, 323.
(27) Weeks, C. M.; Coopre, A.; Norton, D. A. *Acta Crystallogr.* **1969**, *B25*, 443.
(28) Goodman, B. A.; McPhail, B.; Powell, H. K. J. *J. Chem. Soc., Dalton Trans.* **1981**, 822.
(29) This value is significant as compared with the precision (∼0.025 eV) of the energy scan. For nitrogen constituting the complex headgroups the shift of the binding energy line was at most 0.1 eV in the direction opposite to that for copper ions.
(30) The efffect of the *cis*−*trans* isomerization of the ligands around the metal ion in the coordinating compounds of the platinum on the XPS signal was described in a review: Srivastava, S. *Appl. Spectrosc. Rev.* **1986**, *22*, 401.
(31) The variation of the position of the Cu^{2+} binding energy line due to either the water molecule in an apical position or the diastereomeric composition of the complexes was found to be negligible by independent measurements of the crystals of *trans*-Cu(*S*-ala)(*R*-ala)·H_2O, *trans*-Cu(*S*-ala)(*R*-ala),[2] and *trans*-Cu(*S*-ala).[2]
(32) Weissbuch, I.; Popovitz-Biro, R.; Lahav, M.; Leiserowitz, L. *Acta Crystallogr.* **1995**, *B51*, 115.
(33) Guinier, A. *X-ray Diffraction*; Freeman: San Francisco, 1968.